


RESEARCH ARTICLE

A new way to understand migration routes of oceanic squid (Ommastrephidae) from satellite data

Fei Ji¹  & Xinyu Guo²

¹Second Institute of Oceanography, Ministry of Natural Resources, Hangzhou, China

²Centre for Marine Environmental Studies, Ehime University, Matsuyama, Japan

Keywords

Age spectrum, fishing ground distribution, habitat temperature, Japanese flying squid, migration route, VBD satellite data

Correspondence

Fei Ji, Second Institute of Oceanography, Ministry of Natural Resources, Hangzhou 310012, China. Tel: +86 81968507; E-mail: jfmy@sio.org.cn

Funding information

This research is supported by the National Natural Science Foundation of China (42206114).

Editor: Kylie Scales

Associate Editor: David Curnick

Received: 20 January 2023; Revised: 30 July 2023; Accepted: 6 September 2023

doi: 10.1002/rse2.368

Remote Sensing in Ecology and Conservation 2024; **10** (2):248–263

Abstract

Visible Infrared Imaging Radiometer Suite (VIIRS) Boat Detection (VBD) data have been widely used to study the patterns of fishing grounds and their linking to fishery targets, particularly species mainly caught by jiggers. In line with most species in the Ommastrephidae family, the population of *Todarodes pacificus* is made up of various splinter cohorts concerning the timing and location of hatching. Therefore, the satellite-recorded fishing grounds consist of groups with complex age structures and different migration directions within cohorts. This study examined the age composition of harvestable stocks (age spectrum) of *T. pacificus* in the Japan Sea based on an early life history individual-based model of *T. pacificus* and VBD data. Using the age spectrum, we analysed the relationship between fishery effort and the age of the target group. It was found that jiggers most prefer individuals around 310 ± 20 days. Furthermore, the correlation between ambient water temperature and fishing effort revealed that *T. pacificus* migrated to colder waters, reaching the coldest waters at 250 ± 7.5 days before moving back towards warmer waters. We discussed a possible way to use the age-temperature relationship to analyse the flow of VBD distributions to record the movements related to the migration of the fishing target. The results show migration-like trajectories, which are initially parallel to the isotherm, gradually deflect towards lower temperature sides over several months, sharply turn for about a month and then move back with a slight angle to the isotherms. The method provides a potential framework to improve our understanding of the active migration of oceanic squid.

Introduction

Many species of the family Ommastrephidae, also known as oceanic squids, are commercially important to the deep-sea squid jigging and trawling industry. These include *Dosidicus gigas*, *T. pacificus*, *Ommastrephes bartramii* and *Illex argentinus* (Chen et al., 2008; Fukuda & Okazaki, 1998; Yatsu et al., 1999). In 2020, exports of cephalopods reached USD 10.2 billion worldwide, with more than 1/3 comprising species in Ommastrephidae (FAO, 2022). These species have large-scale migrations encompassing thousands of kilometres in their lifespan of 1–2 years (Arkhipkin et al., 2015; Murata, 1990; Nigmatullin et al., 2001). They exhibit a high level of plasticity in their habitat distribution and migration routes, along

with changes in their life history, such as diet, age at maturity and timing of spawning. Therefore, environmental changes have strongly influenced the abundance, distribution and regeneration of fishery stocks, which has resulted in substantial interannual fluctuations in stock size (Rodhouse et al., 2014).

The migration route of oceanic squids is important for efficient fishing operations and fishery stock management. For fishery operations, understanding migration patterns are important in predicting potential fishing grounds. For stock management, the migration route is associated with the growth environment of schooling oceanic squids and is key information in predicting stock size and regeneration. The establishment of banned fishing areas and exclusive economic zones has increased stakeholder focus on changes

in migration routes (Kidokoro et al., 2010; Mokrin et al., 2002). The long migration of oceanic squids is also known for its role in nutrient flow in marine ecosystems (Arkhipkin, 2013; Piatkowski et al., 2001).

Various tracking approaches have been used to examine the migration patterns of oceanic squid. This has included a wide variety of tags (Kidokoro et al., 2010; Rigby & Sakurai, 2005) and biomarkers, such as statolith chemistry analysis, parasite analysis and genetic marker methodologies (Ikeda et al., 2003; Liu et al., 2016; Yamaguchi et al., 2018). Semmens et al. (2007) have systematically reviewed these methods.

In addition to tracking methods based on tagging and nature makers, methods using night-time visible images such as the Defence Meteorological Satellite Program/Operational Linescan System and Visible Infrared Imaging Radiometer Suite Day/night band (VIIRS/DNB) images have increasingly been used in resolving the distribution and migration pattern of harvestable stocks of squid. Most fisheries of Ommastrephidae use light to attract squid, which is convenient for remote monitoring of the migration of Ommastrephidae in oceanic waters through squid fishing fleets (Rodhouse et al., 2001; Semmens et al., 2007). Representative studies include Kiyofuji and Saitoh (2004), Choi et al. (2008), Wei et al. (2018) and Tian et al. (2022), who extracted the migration routes of *T. pacificus* and *O. bartramii* from the centroid transfer of satellite imagery-recorded fishing lights (SIRFL). Waluda and Rodhouse (2006), Alabia et al. (2016), Zhang et al. (2017) and Oh et al. (2020) measured the distribution of SIRFL concerning environmental conditions and estimated the habitat conditions of squid during migration. They reported that water temperature was the most critical environmental factor affecting habitat selection and migration routes.

The SIRFL pattern was assumed to be the approximate distribution of the fishery stock in those studies. The fishing lights were assumed to be a continuous moving set of light spots in satellite images whose trajectory reflects the migration of a squid population. However, some researchers have raised questions regarding this assumption as follows:

1. It is common for multiple groups of squid to migrate simultaneously inside the study area. *T. pacificus* has a distinct autumn-spawning population and a less distinct non-autumn-spawning population dominated by a winter-spawning cohort (Katugin, 2002; Kidokoro et al., 2010). The non-autumn-spawning population comprises splinter cohorts and micro cohorts with variable hatching dates, spawning grounds and migration routes (Takayanagi, 1993; Sakurai et al., 2000). The *O. bartramii* population in the North Pacific encompasses two seasonal cohorts, namely the

winter–spring and autumn-spawning groups (Yatsu et al., 1997). Even if these populations or cohorts have the same migratory strategy, they may show different migratory trends owing to different hatching dates and life stages. Complex motion patterns make it difficult to extract migration patterns at large scales, such as sea basin levels migration trajectories from SIRFL, especially for high temporal resolution data encompassing a relatively large study area. Therefore, Kiyofuji and Saitoh (2004) classified the Japan Sea into seven regions according to temporal variation in fishery lights with the assumption that the fishing activities in each region have been targeted to a specific school of squid. Wei et al. (2018) reduced the research area to ensure that one continuous cohort of fishery targets passed through the research area within a specific timeframe. However, none of these studies has examined how SIRFL corresponds to the diverse selection of multiple age groups. In this study, groups with similar locations, ages and migration trends are referred to as ‘batches’, which constitute a seasonal cohort, to match the high spatiotemporal resolution of satellite data.

2. SIRFL reflects the fishing location of the fleet, that is, the indirect distribution and abundance of fishery effort, and not that of the fishery stock directly (Semmens et al., 2007). Knowledge of fishing and social interaction also affects the distribution of fishery efforts (Barbier & Watson, 2016; Wijermans et al., 2020). Therefore, fishing grounds with equivalent resource abundance may exhibit varying levels of fishery attraction because of the characteristics of targeted species and environmental conditions (Masuda et al., 2014). This study examined how fishermen’s preferences for specific targets such as size influence the distribution of fishing grounds.
3. SIRFL should not move continuously forming a trajectory related to migration. The fishing vessel’s movement is linked to the migration of squid only during the ‘chasing and catching phase’. Therefore, tracking should be interrupted when the chasing phase concludes and transitions into the search or transfer phase between fishing grounds. Otherwise, those movement unrelated to migration may be incorrectly recorded in the trajectories. However, identifying the working phase of a fishing vessel from the movement of the SIRFL is challenging as it is a time-discrete and anonymous record of jigging work location (Oh et al., 2020).

In response to these questions, this study used the age of the harvestable stock as the core variable linking the environmental conditions and the amount of fishery effort, so that fleets can be clustered in respect of the

batch of their fishing target. A similar concept has been well applied to framing the kernel spawning ground of chokka squid (*Loligo reynaudii*) resources in South Africa by utilizing the age distribution to establish a correspondence between hatching events and fishing date (Lipiński et al., 2020). Building upon this concept, we propose several new assumptions for the analysis of SIRFL.1

Assumption

All batches of *T. pacificus* share the same migratory behaviour strategy.2

Assumption

The preference of fishery in catching *T. pacificus* is related to the size of squid. Following Kidokoro et al. (1999) and Arkhipkin and Roa-Ureta (2005), the size of squid is simplified as a unary function of age. For this reason, we assumed the preference of fishery is also a unary function of age.3

Assumption

The movement pattern of the fleets is reflected as a trajectory, only when they chase the schools of a batch of squid. In this scenario, the surrounding environment of the fleet is related to the habit and behaviour of the batch of squid. Otherwise, the vessels in the fleet disperse and enter the search and transfer phase.

This study selected *T. pacificus* as a target, which is the most studied Ommastrephidae species (Rodhouse et al., 2014) with a total annual catch exceeding 300 thousand tons from the 1950s to the 2010s (FAO, 2022). However, this dropped sharply after 2013 and to 22.8 thousand tons in 2018 (Fisheries Agency of Japan, FAJ, 2020). *T. pacificus* has a 1-year life span, which begins with spawning and hatching in the East China Sea and the Japan Sea by following the environmental conditions of 100–500 m in water depth and 19.5–23°C in SST (Rosa et al., 2011; Sakurai et al., 2000). Theoretically, spawning and hatching occur year-round. However, according to the peak hatching abundance, the autumn and winter-spawning cohorts were regarded as the primary fishery stocks (Kasahara, 1978). In the early stage, approximately 140 days after hatching (Ikeda et al., 2003), poor swimming ability allows paralarvae (<45 days) and juvenile (45–140 days) *T. pacificus* to migrate passively with horizontal currents and an ontogenetic vertical migration (Kim et al., 2015). Paralarvae can survive and grow at 15–23°C and the optimum temperature for the juveniles is 10–23°C (Sakurai et al., 1998; Watanabe et al., 1996).

To synthesize these core concepts, an individual-based model (IBM) of the early life stages of *T. pacificus* was developed (Ji et al., 2020). The IBM was verified to be able to estimate the stock size of each batch (Ji et al., 2020) so that we could examine the relationship between multiple batch harvestable stock and SIRFL. This study considered the Japan Sea as the research area because *T. pacificus* resources in the Japan Sea have been strongly exploited (Kasahara, 1978). *T. pacificus* is the dominant species in the Japan Sea, and the traditional fishing method used in the Japan Sea is jigging with a powerful light to attract the squid, leading them to be the major target of fishing boats that use lights in the Japan Sea (Kim et al., 2005; Kiyofuji & Saitoh, 2004). Therefore, selecting the Japan Sea could minimize the underrepresentation of harvestable stock in SIRFL.

Materials and Methods

Given the link between habitat environmental conditions and growth stages, the ambient environment may imply the age of the stock at the specific location (Kishi et al., 2009; Liu et al., 2016). Therefore, the SIRFL data could be analysed according to age information. The conversion of fishery effort into fishery stock and analysis of age-dependent environmental preferences required the age spectrum, which was calculated based on IBM results.

Estimating the age spectrum

IBM (Ji et al., 2020) has been developed to simulate the early life stage of *T. pacificus* from 0 to 140 days for individuals before that age that have poor swimming ability (Ikeda et al., 2003) and can be simulated by our passive migration model. In this model, batches of new individuals were released into the spawning area every 10 days. Consequently, the number and date of each batch of squid surviving for 140 days, that is, joining juvenile stock, could be obtained. The FAJ (2020) reported that the mortality of individuals after the early stage (> 140 days) was relatively constant, that is, $z^* = -0.00582 \text{ day}^{-1}$. We assumed that the stock from each batch was reduced according to the mortality rate for > 140 days.

Todarodes pacificus aged between 180 days to the days before spawning, which was assumed to be 360 days were defined as harvestable individuals (FAJ, 2020). We considered all the surviving individuals within this age range into account as the 'harvestable stock'. We used $r(t, \tau)$ which denotes the amount of harvestable stock at the time t batched by their hatching time τ (Fig. 1A) and have

$$r(t, \tau) = r(\tau + 140, \tau)e^{z^*(t-\tau-140)} \text{ for } t > \tau + 140, \quad (1)$$

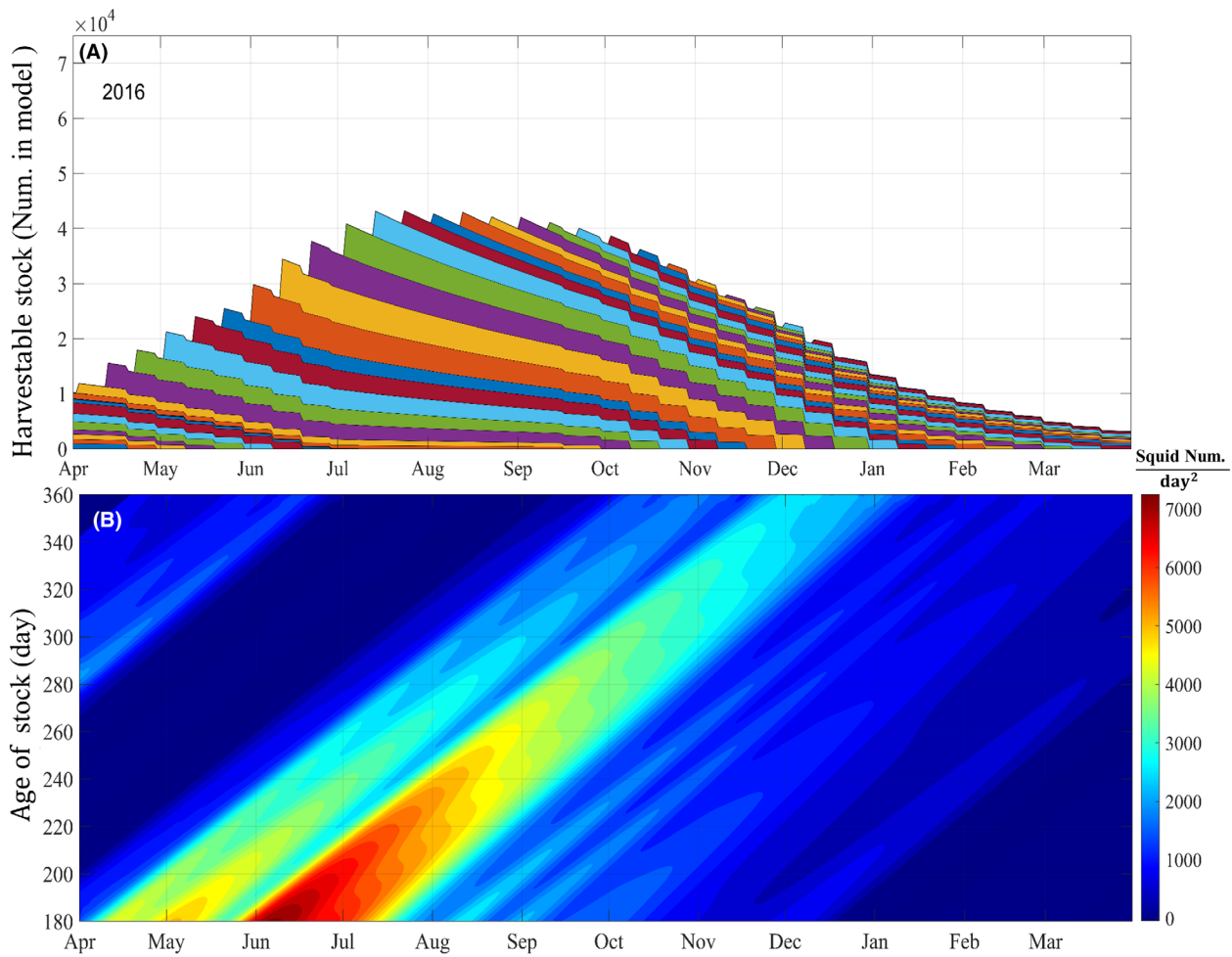


Figure 1. (A) The time series of harvestable stock in 2016 given by the IBM model, which is arranged by hatching dates using different colours. (B) The age spectrum was calculated from (A). The colour represents the stock size (tails of squid) at a specific age (y -axis) on a specific day (x -axis), and the unit is an individual number (result of the model) per day in age per day by date.

where $r(\tau + 140, \tau)$ is the stock size of batch τ at 140 days after hatching, and its value is derived from IBM. In the model calculation, $r(\tau + 140, \tau)$ is output every 10 days to reduce the computational cost. We assumed that the amount of hatching per unit time varied linearly within the 10 days of each interval and used linear interpolation to obtain $r(t, \tau)$ between the two model outputs.

At any instant t , the total amount of harvestable stock contains multiple batches with different hatching times, denoted by τ . Then, the age spectral distribution $S(t, \vartheta)$ can be defined as:

$$R(t) = \int_{t_C}^{t_L} S(t, \vartheta) d\vartheta = \int_{t-t_L}^{t-t_C} S(t, t-\tau) d\tau \quad (2)$$

where ϑ stands for age (days after hatching), t_C denotes the catchable age of squid, which equals 180 days (FAJ, 2020). t_L denotes the lifespan of *T. pacificus*, which is assumed to

be 360 days. $R(t)$ is the amount of harvestable stock. It is relatively simple to obtain the age spectrum $S(t, \vartheta)$ from the IBM result because of $S(t, t-\tau) \equiv r(t, \tau)$, which can be calculated using Equation (1).

Fishing preference

For fishing grounds with the same abundance, the difference in fishery effort invested reflects the preference of fishers. We used Attraction of Stock Per Unit Abundance (ASPA) to quantify the preference of fishermen for a potential fishing ground. ASPA may be influenced by several factors, including economic reasons, quality reasons and individual size. The growth environment may affect the quality of squids, while the season of sale may affect prices. However, as with Assumption 2, for simplicity, ASPA is defined as $F(\vartheta)$, a single-valued function of the

mean age of stock, where ϑ denotes the age of the stock. Without loss of generality, we used a Gaussian formal function $F(\vartheta)$:

$$F(\vartheta) = B_1 \exp\left(-B_2(\vartheta - \vartheta_{\text{opt}})^2\right) \quad (3)$$

B_1 reflects the ratio of stock size to fishery effort, B_2 reflects the breadth of fishing preference in age and ϑ_{opt} reflects the optimal age of fishing preference. We conducted a regression analysis to find the undetermined coefficients using age data and fishery effort data.

The fishing attraction in the study area, that is, the Japan Sea, is

$$A(t) = \int_{t_c}^{t_L} S(t, \vartheta) F(\vartheta) d\vartheta \quad (4)$$

Given that the resources of *T. pacificus* in the Japan Sea have been strongly exploited (Kasahara, 1978), the amount of fishery effort shown by SIRFL is assumed to be proportional to the attraction in the Japan Sea.

$$E(t) = KA(t) \quad (5)$$

Here, $E(t)$ represents the fishery effort. We used the number of boats reported by the VBD in the Japan Sea as the value of $E(t)$. K is the scale factor between attraction and fishery effort, which can be combined into coefficient B_1 . Then we have:

$$E(t) = B_1 \int_{t_c}^{t_L} S(t, \vartheta) \exp\left(-B_2(\vartheta - \vartheta_{\text{opt}})^2\right) d\vartheta \quad (6)$$

Therefore, we established the relationship between the known time-series fishery effort $E(t)$ and the age spectrum $S(t, \vartheta)$. There are three constants (B_1 , B_2 and ϑ_{opt}) to be determined. Owing to the large interannual variation in stock size, we determined the set of constants annually. Using the daily VBD data, 365 or 366 samples were collected from the 2012 to 2019 fishing year to determine the three coefficients for that year using the nonlinear regression method. In this way, the ASPA expression $F(\vartheta)$ is obtained for each year, which quantitatively describes the change in fishery preference with the age of the target squid. If the age structure in a certain fishing ground is known, $F(\vartheta)$ gives the transformation relationship between the stock abundance and fishery effort.

Age-dependent most-preferred habitat temperature (APHT)

Habitat temperature is influenced by two factors, namely how squid schools select habitat environments through positive migration and local environmental change caused by oceanographic processes (Liu et al., 2016). We defined

variable T_h as the habitat temperature, described using a linear model of temperature preference and environmental temperature as follows:

$$T_h(\vartheta, t, \mathbf{x}) = \alpha T_{\text{adapt}}(\vartheta) + \beta T_{\text{Sea}}(t, \mathbf{x}) + \beta_0 \quad (7)$$

$T_{\text{adapt}}(\vartheta)$ represents the temperature preference during the growth of individuals. Based on Assumption 1, different squid batches may behave differently. However, their migration patterns, that is, the reaction to surrounding environmental conditions, remain consistent within the same life stage. Therefore, T_{adapt} is a univariate function of age (ϑ). According to the Ca: Sr. ratio analysis of statoliths by Ikeda et al. (2003), the ambient temperature experienced by *T. pacificus* in the Japan Sea can be modelled as a quadratic function of age, with C_0 , C_1 and C_2 denoting the 0th-, 1st- and 2nd-order coefficients of age concerning growth temperature, respectively.

$$T_{\text{adapt}}(\vartheta) = C_2 \vartheta^2 + C_1 \vartheta + C_0 \quad (8)$$

$\beta T_{\text{Sea}}(t, \mathbf{x}) + \beta_0$ in Equation (7) represents the impact of environmental changes on individuals within the region, where \mathbf{x} represents the location of the habitat and β and β_0 are the affine type parameters of the environmental temperature condition of the local habitat.

Applying a spatial average encompassing the Sea of Japan to Equation (7), we obtain

$$\overline{T}_h(\vartheta, t) = \overline{T}_{\text{adapt}}(\vartheta) + \beta \overline{T}_{\text{Sea}}(t) \quad (9)$$

where the overbar indicates the spatial average across the Japan Sea. This is to eliminate the influence of the local temperature. The average habitat temperature selected by the *T. pacificus* of age ϑ at time t is represented by $\overline{T}_h(\vartheta, t)$, which is linked to its temperature preference during the growth of individuals across the Japan Sea ($\overline{T}_{\text{adapt}}(\vartheta)$) and the spatial average of the upper water temperature in the Japan Sea. In this calculation, α is incorporated into C_2 , C_1 , C_0 and β_0 are incorporated into C_0 .

To determine the parameters of the APHT model for the Japan Sea, we used the model to fit the average ambient water temperature link to the SIRFL-indicated fishing fleets. Given that the selection of fishing grounds is affected by fishing preferences, the average water temperature of the fishing ground needs to consider the weighting of the fishing preferences by age. This should correspond to the ASPA ($F(\vartheta)$ in 2.2), which is the function of the age spectrum ($S(t, \vartheta)$) and ASPA ($F(\vartheta)$):

$$\overline{T}(t) = \frac{\int_{t_c}^{t_L} S(t, \vartheta) F(\vartheta) \overline{T}_h(\vartheta, t) d\vartheta}{E(t)} \quad (10)$$

where $S(t, \vartheta)$, $F(\vartheta)$ and $E(t)$ have been given in subsections 2.1 and 2.2 respectively, which are known

conditions. $\bar{T}(t)$ is the average temperature of the fishing ground which was averaged from the distribution of the SIRFL and water temperature data at those locations. We perform regression analysis on the time-dependent average ambient temperature linked to SIRFL to determine the undetermined coefficients, C_0 , C_1 , C_2 and β in Equation 10.

Habitat temperature-associated chasing patterns extraction from SIRFL

The schools of squid migrated continuously and their ambient environmental conditions gradually changed. Therefore, we used a continuous function (Equation 7) to reflect the relationship between habitat temperature and squid age. Based on Assumption 3, the ambient temperature of fleets reflects the environmental conditions of the targeted batch of squid during their chasing and catching phase. In contrast, abrupt changes in environmental conditions suggest a switch of target batch.

We performed a temporal analysis of the vessels' distribution in VBD and their correlation with ambient temperature. Based on proximity within the temperature–time state space, vessels were clustered into fleets, which exhibited distinct ridge patterns as they conducted chasing and catching activities. By identifying persistent ridges over time, vessels in the VBD dataset were labelled according to their respective temperature bands, which indicated membership within specific fleets.

We assessed the ridges as chasing and caught the movement of the fleet by analysing the gradient of the crest line within a range of $\pm 0.2^\circ\text{C}/\text{day}$. The threshold was determined through Equation 7 using parameters from Table 2 and considered the typical gradient of the polar front in the Japan Sea ($0.03^\circ\text{C}/\text{km}$ Park et al., 2004) as well as the representative migration speed of Ommastrephidae (30 km/day, Gilly et al., 2006). By geographically mapping the labelled fleets and adjusting with geographic distance, we obtained the movement pattern of the fleet during the duration of chasing a batch. The trajectory of the fleet was approximate to the migratory trajectory of the fishery targets.

Data

We used the VBD product offered by NOAA's earth observation group as the data source for our batch-by-batch analysis of SIRFL (Elvidge et al., 2015). This dataset has been validated against the Automatic Identification System and vessel monitoring system data (Elvidge et al., 2018, 2022). Within the Japan Sea, the abundance and distribution of VBD have been shown to match effectively with those of the jigging vessels (Oh et al., 2020). We used the

daily VBD data from April 2012 to March 2020 and only high-feasibility detections (whose quality flag = 1 in Elvidge et al., 2015) were included in our analysis.

The CPUE data acquired by the fishing synchronous survey are presented in FAJ (2020).

The temperature or temperature gradient (front strength) is the most important environmental variable controlling the migration of Ommastrephidae (Alabia et al., 2016). We used water temperature data provided by the JCOPE2M (Japan Coastal Ocean Predictability Experiment) assimilation system, which uses a multi-scale 3-dimensional variational method (Miyazawa et al., 2017; Sil et al., 2012). Given the ontogenetic vertical migration, *T. pacificus* stays at a depth of approximately 100 m during the daytime and reaches the surface to prey at night (Yamamoto et al., 2007). Therefore, we determined the vertical-averaged temperature at 0–100 m in depth as a reference condition for migration.

Results

Age spectrum

Figure 1A shows the harvestable stock size in the 2016 fishing year from 1 April 2016 to March 31, 2017, arranged by hatching date. We have shown data from 2016 as an example year, with other data available in the supplementary materials. From April to the end of June, the harvestable stock size increased steadily with the addition of multiple batches of individuals. July to September was the peak period in terms of stock size, during which the decline and replenishment of stocks were balanced. From October to the end of December, the stock size steadily decreased as the autumn spawning cohort entered the spawning stage and then died. By the end of December, the amount of harvestable stock was approximately one-quarter of its peak. From January to March of the following year, the winter-spawning cohort entered the spawning stage and then the stock decreased to the minimum size for the entire fishing year. This seasonal variation was consistent with the annual variation in CPUE obtained from a synchronous fishing experiment by FAJ (2020) (Fig. 2A).

The age spectrum (Fig. 1B) was created by counting the squid stock size based on their age, which shows a ridge of high value with a slope close to one because of synchronous increase in age and time. Given the stock size decreased proportionally with time, its value was lower on the higher age side than on the lower age side along the ridge. New batches were added to the harvestable stock intensively from May to June (Fig. 1B), with the batch added in June being the largest. These batches were from autumn-hatched cohorts from November to

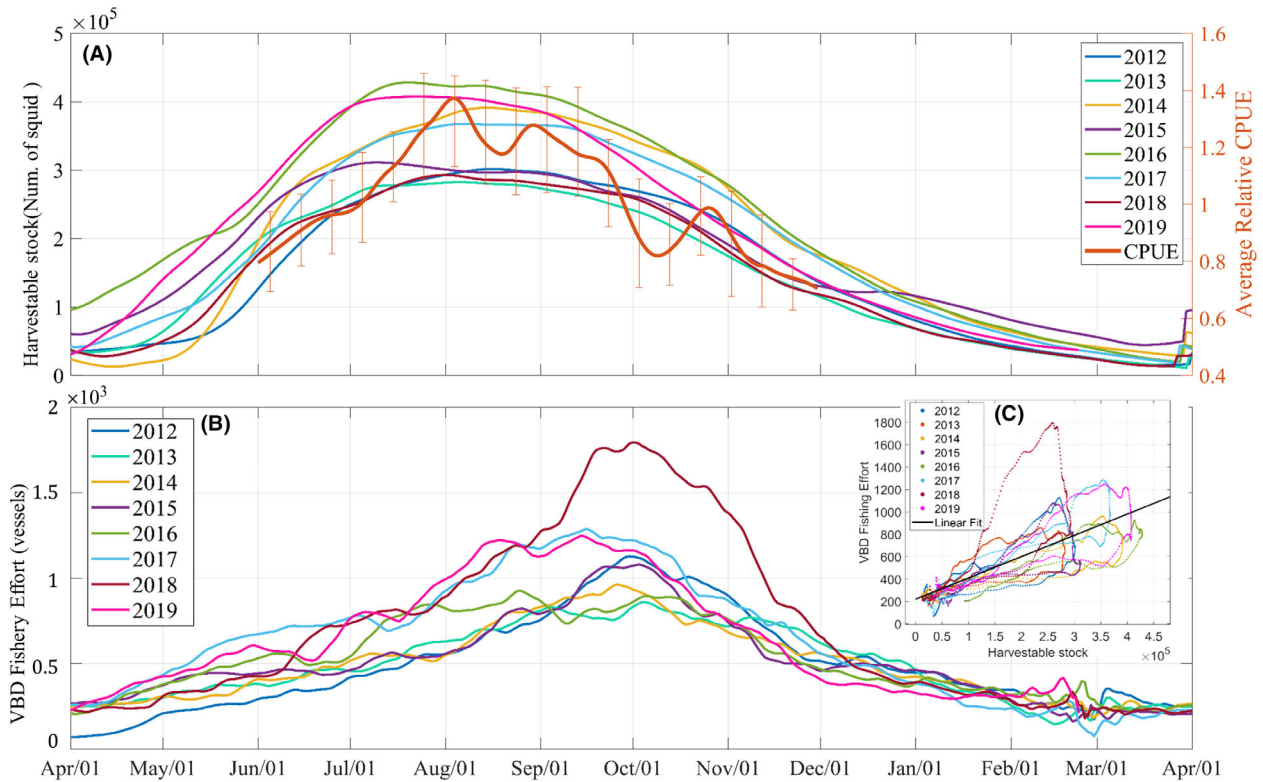


Figure 2. (A) Time series of stock size in the Japan Sea derived from the IBM model (Ji et al., 2020) and that of CPUE (FAJ, 2020). (B) Time series of harvestable fishery efforts reflected by SIRFL. (C) Scatter plot between the harvestable stock size from the IBM model and the fishery effort from SIRFL.

December of the previous year. The batch size of the newly added harvestable stock from July to October gradually decreased to half of the peak value, which corresponded to the batch size of the winter-hatched cohorts.

The age spectrum reflected changes in the age of the harvestable stock during the year. Most harvestable squids were younger individuals between 180 and 220 days in June and July. From August to November, most of the stock comprised individuals over 240 days old. The differences in age composition among months offered the potential of explaining the variations in fishery effort during the year using age preferences in fishing.

Age preferences in fishing

The harvestable stock size time series estimated by the IBM model and the observed CPUE showed consistent variation throughout the year (Fig. 2A). The peak harvestable stock size was reached from July to September and declined from October until the end of the fishing year. The lowest stock size period was from December to April. In contrast, the peak of fishery efforts detected by SIRFL was recorded from August to September (Fig. 2B).

There was a lag of approximately 1.5 months between harvestable stock and fishery effort.

The fishing age preference model (Equation 6) was fitted using the time series of harvestable stock size for each year (Fig. 2A) and the amount of fishery effort indicated by the SIRFL (Fig. 2B). Figure 3A shows the results of the age preference model, where the ASPA changes with the average age of stock of *T. pacificus* in the Japan Sea. The parameters obtained for each year are shown in Table 1.

Parameter B_1 represents the proportional coefficient of the ASPA converted to the fishery effort. There was little difference in B_1 for each year, except for the 2018 fishing year. This indicates that the fishery effort invested in fishing grounds based on fishing preferences in the Japan Sea has been relatively stable in most years, and we could undertake a conversion between stock size and fishery effort based on ASPA. In the 2018 fishing year, B_1 was more than twice as high as in the other years because of the higher fishery effort in 2018 (Fig. 3C). However, the reason for this is not clear. ∂_{opt} indicates the most popular age at which the most squid was harvested. The optimal age for all years was 310 ± 20 d.

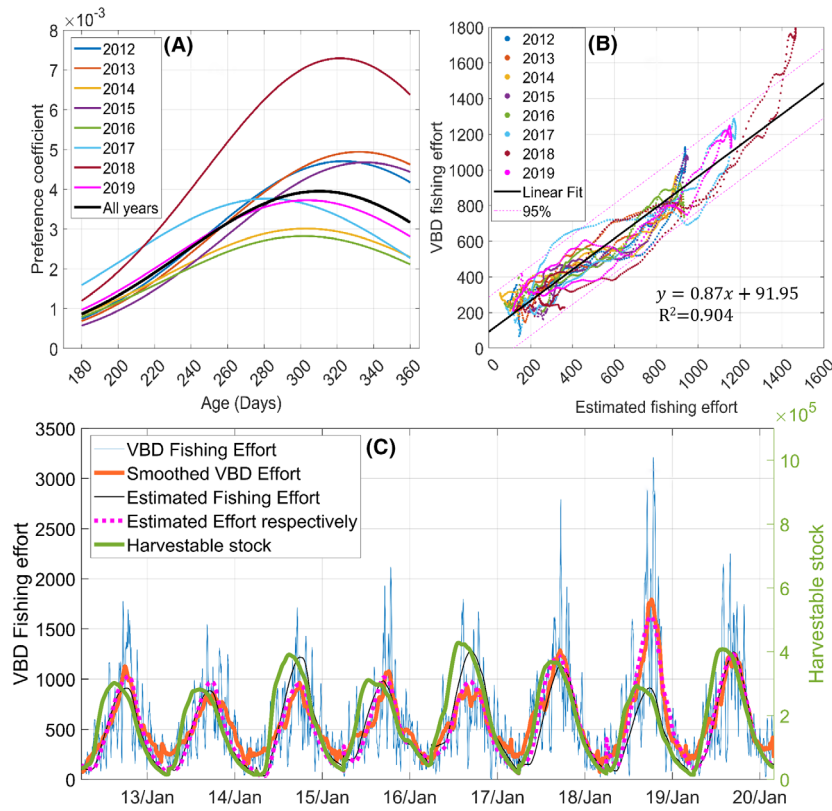


Figure 3. (A) Variation in ASPA with age. (B) Scatter plot of the estimated fishery effort by fishing preference model and SIRFL (VBD) data. (C) Comparison between the time series of fishery effort indicated by VBD and the fishery effort calculated from the fishing preference model. As an input variable to the model, the harvestable stock time series is plotted with the green line with referring to the right ordinate.

Table 1. Parameter regression results using the fishing preference model (Equation 6).

Fishing year\parameters	B_1	B_2	ϑ_{opt}
2012	4.71×10^{-3}	8.97×10^{-5}	323.376
2013	4.94×10^{-3}	8.52×10^{-5}	331.974
2014	3.02×10^{-3}	8.37×10^{-5}	302.925
2015	4.68×10^{-3}	8.69×10^{-5}	335.336
2016	2.82×10^{-3}	8.55×10^{-5}	301.856
2017	3.77×10^{-3}	8.27×10^{-5}	281.994
2018	7.29×10^{-3}	9.02×10^{-5}	321.427
2019	3.73×10^{-3}	8.82×10^{-5}	303.544
Fitted for all years	3.95×10^{-3}	8.68×10^{-5}	310.299

B_1 represents the proportional coefficient of the ASPA converted to the fishery effort. Parameter B_2 determines the decay rate of the ASPA on both sides of the preferred age group. ϑ_{opt} indicates the age at which the most-preferred squid was harvested.

Parameter B_2 determines the decay rate of the ASPA on both sides of the preferred age group. The average value was approximately 8.5×10^{-5} , and the relative variation was <7% in all years. With conversion, the ASPA of individuals with an age of 180 days was approximately

0.19 times that of individuals with the age of ϑ_{opt} . Figure 3B and C show the relationship between the fishery effort recorded by the VBD data and the fishery effort calculated by the fishing preference model based on the estimated values in Table 1. The results have shown that the model can effectively reproduce the variation pattern of fishery effort recorded in the VBD data.

Habitat transfer with age

Figure 4A shows the variation in $T_{adapt}(\vartheta)$ with the age of *T. pacificus*. C_0 in $T_{adapt}(\vartheta)$ also contains a constant owing to environmental changes. The changes in β_0 could not be separated, which may have induced interannual variability in the baseline of $T_{adapt}(\vartheta)$. However, the seasonal variation of $T_{adapt}(\vartheta)$ is credible and reflects the temperature variation caused by autonomous decision-making in the migration process.

The APHT model predicts that *T. pacificus* migrates to colder regions from 180 days, reaches the coldest region at approximately 250 days and then migrates to warmer regions (Fig. 4A).

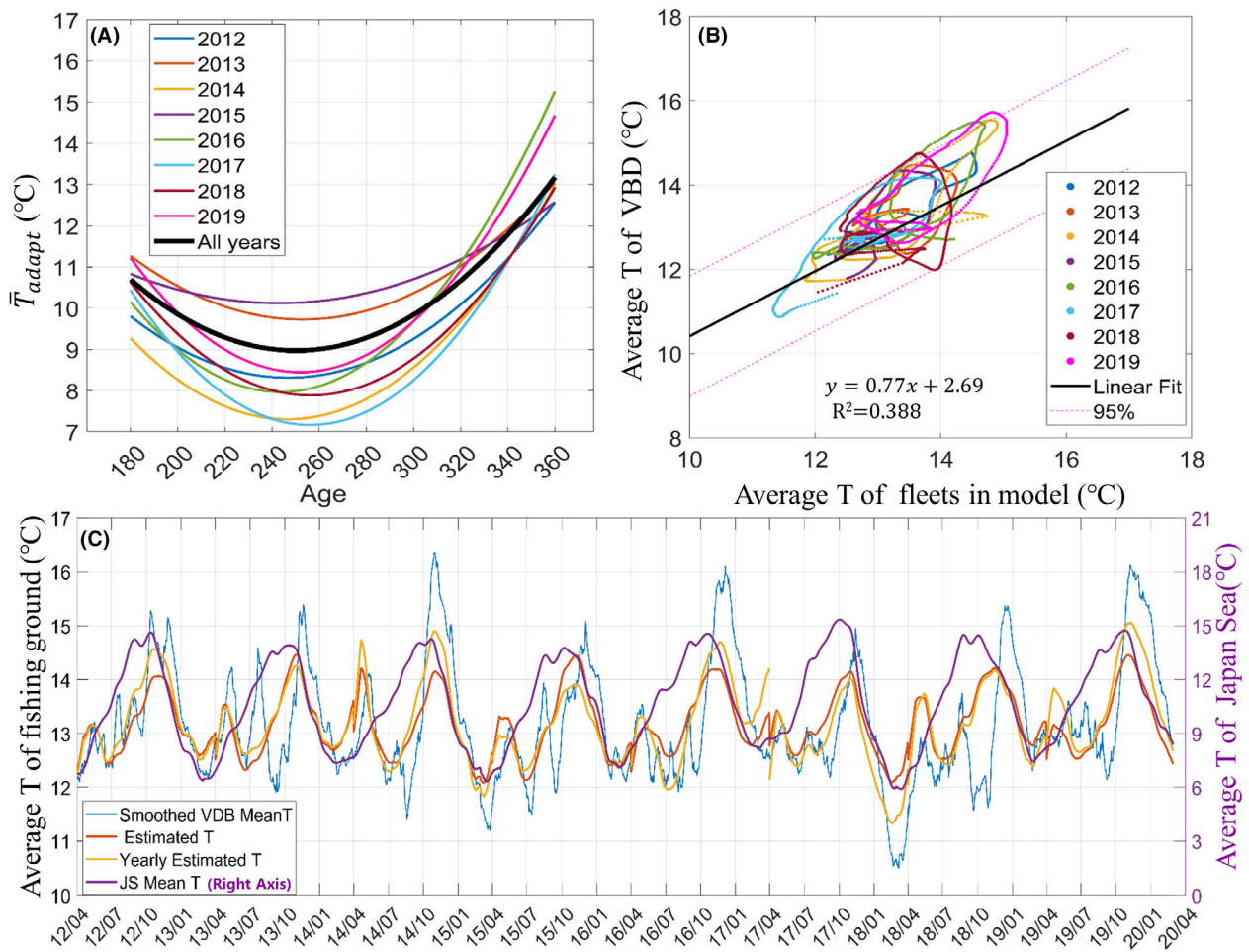


Figure 4. (A) Ambient temperature change because of the habitat of individuals ($T_{adapt}(\theta)$) with age. (B) Scatter plot between the APHT model result and the water temperature recorded on the fishing set. (C) Comparison between the time series of water temperature on the fishing set indicated by VBD data (blue curve) and water temperature estimated by the APHT model. The orange curve used the same parameters (bottom line of Table 2) for all years, while the yellow curve used the parameters varied from year to year (Table 2). The purple curve represents the average water temperature in the Japan Sea, which is used in the model to represent the environmental effect on the fishing set and has a reference shown at the right coordinate axis.

Based on the APHT model and fishing preferences, we used Equation 10 to generate time series of the average temperatures for the Japan Sea fishing grounds (Fig. 4C). The result based on yearly change parameters from Rows 2 through 9 of Table 2 partially replicates the temperature pattern of the fishing ground, which exhibits a bimodal structure throughout the year with peaks in May/June and November, at approximately 14.5°C and a low point in July/August at approximately 12°C.

Using the same parameters for all years from 2012 to 2019 corresponding to the parameter at the bottom line of Table 2, the APHT model could still reproduce this pattern. This suggested that the model was stable in different years, although the stock size and catch changed substantially in

those years. The fitness between the model results and satellite-based observations is shown in Figure 4B and the R-square coefficient of linear regression is 0.388, which indicated that the model could partially explain the variation in the average temperature of the fishing ground.

The temperature variation in the fishing ground was significantly different from that of the average temperature in the Japan Sea (blue curves in Fig. 4C). The average temperature of the upper 100 m layer in the Japan Sea reached its lowest at approximately 7°C in March–April and the highest at approximately 15°C in August–October annually, representing a difference of approximately 8°C. This is greater than the temperature change in the fishing ground.

Table 2. Results of parameter estimation in the *Todarodes pacificus* habitat temperature model (Equation 9).

Fishing year	C_2	C_1	C_0	β	$-C_1/2C_2$
2012	0.333×10^{-3}	-0.164	28.600	0.355	246.25
2013	0.290×10^{-3}	-0.147	28.281	0.234	253.45
2014	0.442×10^{-3}	-0.218	34.203	0.414	246.61
2015	0.179×10^{-3}	-0.087	20.710	0.203	243.02
2016	0.539×10^{-3}	-0.263	39.981	0.300	243.97
2017	0.564×10^{-3}	-0.289	44.205	0.359	256.21
2018	0.470×10^{-3}	-0.241	38.800	0.337	256.38
2019	0.534×10^{-3}	-0.269	42.405	0.307	251.87
Fitted for all years	0.349×10^{-3}	-0.175	30.842	0.276	250.72

C_0 , C_1 and C_2 denote the 0th-, 1st- and 2nd-order coefficients of age with respect to growth temperature, respectively. β stand for the influence coefficient of the environment on the individual. The last column denotes the age corresponding to the lowest temperature point.

Fleet tracking using auxiliary information on ambient temperature

Figure 5A depicts the temporal pattern of fishing vessels in VBD in 2016. The density of fishing vessels exhibits a strong tendency to accumulate in a specific temperature band under the temperature coordinate. Despite an apparent temporal discontinuity, the trend of bands' continuous evolution over time became evident. Figure 5B illustrates the density ridges that emerged after applying temporal filtering to eliminate interval disruptions in the bands.

The ridges in Figure 5B could be divided into three groups. Group 1 is active in waters between 5 and 10°C, with ridges appearing at approximately 5°C in May and June. The density of vessels increased rapidly as the temperature rose to approximately 7°C from August to

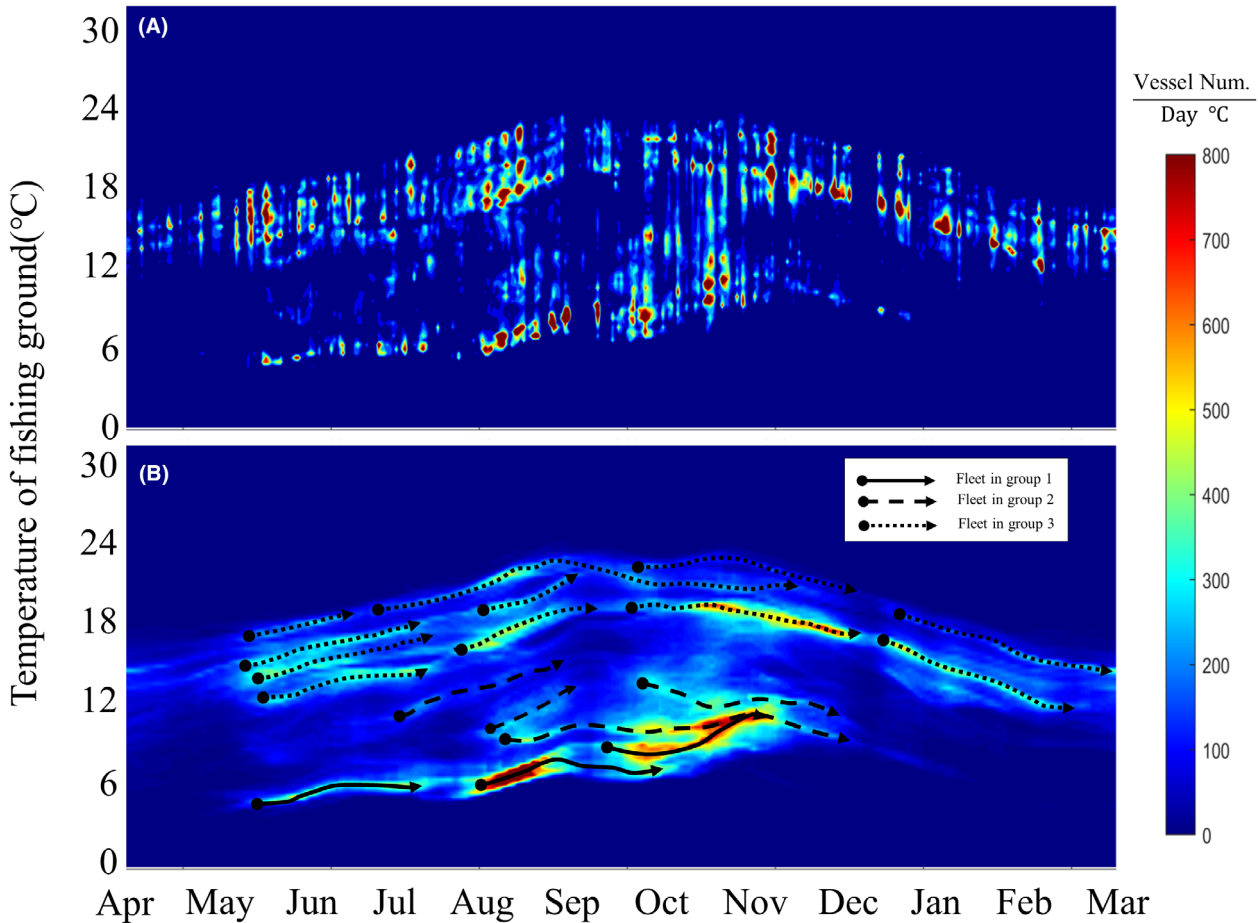


Figure 5. (A) Time series of the VBD fishery effort distributed by the water temperature of the fishing set. (B) Same as (A) but after a 30-day running mean, the highlighted ridges in (A) represent continuous temperature changes where fishery effort has been concentrated. The clustering of the fishing vessels based on the age-temperature relation and special distance is denoted by a dotted arrow line. Each cluster represents a potential fleet that chases and catches fishery targets from a batch. The initiation of a chase is denoted by solid dots, while the conclusion of the chase is indicated by arrows.

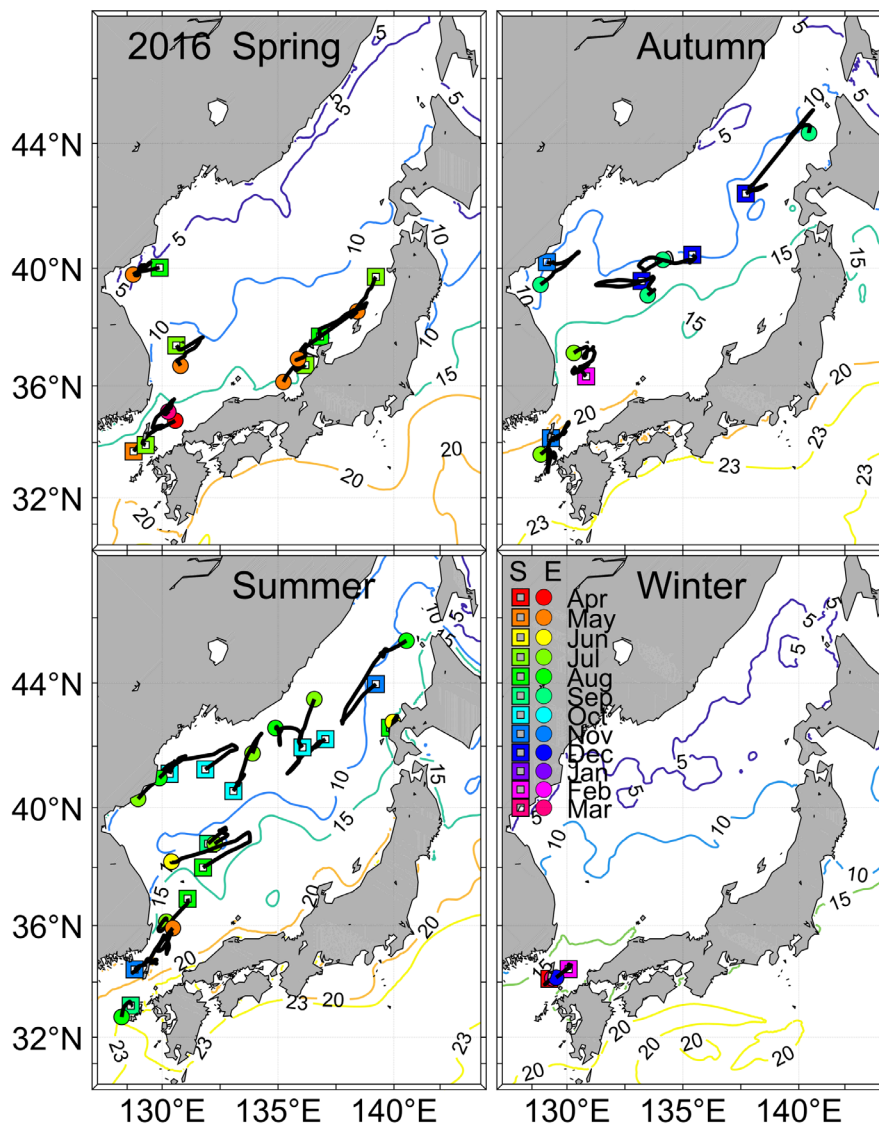


Figure 6. The trajectory of 'fleets' processed from VBD data. Taking 2016 as an example, the trajectories are divided into four panels according to the season of occurrence. The solid black line represents the daily trajectory of a cluster fishing boat, which reflects the migration of schools of *Todarodes pacificus*. The dot and triangle marks represent the position of the centre of the cluster in the corresponding month. The triangle marks are the starting positions of the trajectories where the fishing boat began to catch *T. pacificus* from that school. The dot marks are the position of the trajectory on the first day of that month. The colour of the markers denotes the specific month. The background contour lines indicate the average water temperature of the upper 100 m layer.

September. By November, the ridges reached approximately 10°C before gradually dissipating around December. Group 2 formed between the 10 and 15°C isotherm in July and August, gradually moved to lower temperatures and merged with Group 1 in October–November. Group 3 consisted of several ridges that maintained a fixed temperature difference, appearing from May to next January with a temperature variation between 12 and 24°C. This was synchronized with the annual change in

water temperature around the Tsushima Strait. The vessel density was highest from August to November.

The movement trajectory of the fleets is depicted in Figure 6, exhibiting a distinct seasonal distribution. In spring, the fleets are usually found in three areas, that is, along the Korean Peninsula coast at around 40 degrees north latitude with temperatures of approximately 5°C, on the western side of Honshu Island in Japan (10–15°C) and in the Tsushima Strait (> 15°C). These

corresponded to Groups 1, 2 and 3, respectively. Group 3 remained near the Tsushima Strait for four seasons. During summer, fleets from Group 1 moved eastward along the 7°C isotherm to reach the sea south of Primorsky, Russia. Group 2 was found near the 10°C isotherm and around the shelf area located at 130–134°E and 38°N west of Hokkaido, Japan. In autumn, Group 1 shifted southward to merge with Group 2 near the 10°C isotherm, forming fishing grounds across the northern Japan Sea. In winter, both groups disappeared.

There was a consistent pattern in the trajectories of all fleets, characterized by a gradual move towards the cooler water with a slight angle to the isotherm before making a sharp turn towards the warmer water that remained for approximately 2–4 weeks before the chasing activity concluded. This trend was observed across all three groups during all four seasons, with a particular emphasis on Groups 1–2. Most fleets examined in this study continued the chasing phase for 2–3 months.

Discussion

We considered the relationship between fishery lighting and the stock of squid using a new method. The jigger interest in squid varied by age, with individuals around 310 days old attracting the most effort, while older and younger stocks became less attractive. This is consistent with Murata (1990) that fishermen prefer to catch immature squid of larger size. It is uncertain whether the fishermen acted intentionally, but their long-established fishing practices appear to have the preference for squid.

If it is acknowledged that the fleet's pursuit is age-specific, once a certain batch of squid has been harvested, the fleet lacks the incentive to accompany the fish through their life history. It appears more strategic to move directly to the next fishing ground for potential fishery stocks. Similarly, the fleet did not track underage schools. Therefore, it is unlikely that the annual movement of the fishing ground where fishing effort is concentrated could reflect the migration trajectories of a cohort of squid throughout their entire life history. However, many studies have depicted the migration by tracking the movement of the fishing grounds (Murata, 1990; Kiyofuji & Saitoh, 2004; Choi et al., 2008; Wei et al., 2018; Tian et al., 2022).

In our understanding, squid of different batches were caught at a specific age. The fleet moved and followed the migration of target squid during the chasing and catch phase, which usually lasted for 2–3 months (Fig. 5B). However, the catch timing and location of batches varied according to season, resulting in an annual cycle in the location of fishing grounds (Choi et al., 2008; Murata, 1990) Given that *T. pacificus* hatches throughout the

year, likely, the location of fishing moves continually along specific routes.

Our analysis (Fig. 6) has shown that the fleet's chasing positions and timing was consistent with the fishing grounds as summarized by Murata (1990). However, we did not estimate the migration path according to the order of these fishing grounds following the methods of Murata (1990), Kiyofuji and Saitoh (2004) (Figures S1 and S2). *T. pacificus* in the Japan Sea can be divided into two groups according to its migration path, initial migration along the coast of Japan (Tsushima group) and the Korean peninsula (subarctic group) (Kim et al., 2015; Kishi et al., 2009). The path examined by Choi et al. (2008) likely comprised the migration of the subarctic group. Our results showed that the fleets fishing in two distinct groups corresponded to the migration paths identified by Kishi et al. (2009). The fishing grounds for Group 1 were distributed along the path of the subarctic group, and Group 2 was distributed along the path of the Tsushima group.

In our results, fleets within a group exhibited their independent moving trajectories, all of which conformed to the pattern of moving towards colder waters before transitioning to warmer areas. This suggested that squid undergo similar migratory movements during their fishing stage and are likely caught at similar ages. These observations aligned with the assessment of changes in growth environments by Ikeda et al. (2003) based on statolith analysis.

Statolith analysis does not provide the absolute value of growth temperature. Therefore, we estimated the specific range of the temperature-based APHT model (Fig. 4A). The temperature gradient experienced by *T. pacificus* during migration, ranged from 8.5 to 13.5°C, after removing the environmental background temperature. This is suitable for *T. pacificus* migrating across the polar front area in the Japan Sea, which has a temperature difference of approximately 5°C across the front (Park et al., 2004). This temperature pattern has been maintained throughout 2012–2019 and was consistent with the pattern presented by Ikeda et al. (2003).

The calculation of the age spectrum was based on the stock of 140 days-old individuals of IBM (Ji et al., 2020) and the fixed mortality coefficient, which is consistent with the statistical calibre of FAJ. To validate the age spectrum, we used a report of age calculated from statoliths (Sakaguchi et al., 2009) and the average mantle length of captures (FAJ, 2020, Appendix S2) to estimate the annual variation pattern of their mean age. The comparison between the age spectrum-based capture age and FAJ records indicated a close fit; the age distribution based on statolith is close to our age spectrum in terms of mean age and peak date, providing further support for our findings (Appendix S1).

To date, the fisheries effort data in VBD has lacked verification from the northern part of the Japan Sea, which is analogous to that in the southern part. There were unusually high values recorded between September and October 2018. The high density of vessels observed in the offshore waters of Primorsky, Russia, north of latitude 42°N in September 2018 accounted for 26% of the total annual detections of 2018. Likely, this is not a false positive in the satellite data, but rather an unknown eventful process not closely related to the main conclusions of our study.

Conclusions

In this study, a new idea was proposed for processing satellite-recorded fishery data, which has introduced information on the habits and age composition of fishing targets. This information is likely to regulate the habitat selection of the target fish and the investment of effort from fishing vessels. Our method helped us to establish a link between the abundance of fishing vessels and Ommastrephidae resources. The results suggested that the relationship between fishing effort and harvestable stock size could be estimated from the age spectrum, which was also found to be related to the temperature conditions of the fishing grounds. The age of the target fish could then be inferred based on these temperature conditions.

We used inferred age information from the *T. pacificus* targeted based on environmental conditions to cluster fleets in VBD data. By tracking those fleet movements, we obtained a likely migration trajectory for the *T. pacificus* targeted. This method allowed for the examination of migration patterns at the batch level, rather than a cohort level in previous research. This has the potential to facilitate further research on the relationship between environmental conditions and migration patterns. It avoids anchoring migration trajectories solely based on latitude and longitude coordinates without considering feedback to environmental changes. An IBM model with active migration processes could be developed based on this study to quantitatively analyse how changes in environmental conditions affect the entire life cycle of Ommastrephidae. For instance, the spawner–recruit relationship variation of *T. pacificus* during regime shifts (Nishijima et al., 2021) may be attributed to alterations in reproductive migration patterns influenced by climate change.

Author Contributions

Conceptualization, Fei Ji and Xinyu Guo; methodology, Fei Ji and Xinyu Guo; software, Fei Ji; validation, Fei Ji; formal analysis, Fei Ji; investigation, Fei Ji; resources, Fei Ji and Xinyu Guo; data curation, Fei Ji; writing—original

draft preparation, Fei Ji and Xinyu Guo; writing—review and editing, Fei Ji and Xinyu Guo; visualisation, Fei Ji; supervision, Xinyu Guo; project administration, Xinyu Guo; funding acquisition, Fei Ji. All authors have read and agreed to the published version of the manuscript.

Acknowledgements

We would like to thank the Fisheries Research Agency of Japan for sponsoring a series of works that share the fishing record and stock data of Japanese flying squid. This research is supported by the National Natural Science Foundation of China (42206114).

Data Availability Statement

Daily VBD data can be accessed at https://eogdata.mines.edu/eog/EOG_sensitive_contents. Resource evaluation of Japanese flying squid by the Fisheries Research Agency of Japan can be accessed at <https://abchan.fra.go.jp/index.html>. The rest of the data used in this paper including the result of the IBM model and the age spectrum will be uploaded to the publisher's server for open access.

References

- Alabia, I., Dehara, M., Saitoh, S.-I. & Hirawake, T. (2016) Seasonal habitat patterns of Japanese common squid (*Todarodes pacificus*) inferred from satellite-based species distribution models. *Remote Sensing*, **8**, 921.
- Arkhipkin, A.I. (2013) Squid as nutrient vectors linking Southwest Atlantic marine ecosystems. *Deep Sea Research Part II: Topical Studies in Oceanography*, **95**, 7–20.
- Arkhipkin, A.I. & Roa-Ureta, R. (2005) Identification of ontogenetic growth models for squid. *Marine and Freshwater Research*, **56**(4), 371–386.
- Arkhipkin, A.I., Rodhouse, P.G.K., Pierce, G.J., Sauer, W., Sakai, M., Allcock, L. et al. (2015) World squid fisheries. *Reviews in Fisheries Science & Aquaculture*, **23**, 92–252.
- Barbier, M. & Watson, J.R. (2016) The spatial dynamics of predators and the benefits and costs of sharing information. *PLoS Computational Biology*, **12**, e1005147.
- Chen, X., Liu, B. & Chen, Y. (2008) A review of the development of Chinese distant-water squid jigging fisheries. *Fisheries Research*, **89**(3), 211–221.
- Choi, K., Lee, C.I., Hwang, K., Kim, S.W., Park, J.H. & Gong, Y. (2008) Distribution and migration of Japanese common squid, *Todarodes pacificus*, in the southwestern part of the East (Japan) Sea. *Fisheries Research*, **91**(2–3), 281–290.
- Elvidge, C., Zhizhin, M., Baugh, K. & Hsu, F.-C. (2015) Automatic boat identification system for VIIRS low light imaging data. *Remote Sensing*, **7**, 3020–3036.
- Elvidge, C.D., Ghosh, T., Baugh, K., Zhizhin, M., Hsu, F.C., Katada, N.S. et al. (2018) Rating the effectiveness of fishery

- closures with visible infrared imaging radiometer suite boat detection data. *Frontiers in Marine Science*, **5**, 132.
- Elvidge, C. D., Ghosh, T., Hsu, F. C., & Zhizhin, M. (2022). VIIRS Monitoring and Reporting on Lit Fishing Vessel Detections in Southeast Asia. In IGARSS 2022–2022 IEEE International Geoscience and Remote Sensing Symposium (pp. 4779–4782).
- FAO. (2022) *The State of World Fisheries and Aquaculture 2022. Towards Blue Transformation*. Rome: FAO. Available from: <https://doi.org/10.4060/cc0461en>
- Fukuda, Y. & Okazaki, E. (1998) Current situation on utilization and its related research of squid in Japan. In: Okutani, T. (Ed.) *Contributed papers to international symposium on large pelagic squids*. Tokyo: Japan Marine Fishery Resources Research Center, pp. 261–268.
- Gilly, W.F., Markaida, U., Baxter, C.H., Block, B.A., Boustany, A., Zeidberg, L. et al. (2006) Vertical and horizontal migrations by the jumbo squid *Dosidicus gigas* revealed by electronic tagging. *Marine Ecology Progress Series*, **324**, 1–17.
- Ikeda, Y., Arai, N., Kidokoro, H. & Sakamoto, W. (2003) Strontium: calcium ratios in statoliths of Japanese common squid *Todarodes pacificus* (Cephalopoda: Ommastrephidae) as indicators of migratory behavior. *Marine Ecology Progress Series*, **251**, 169–179.
- Japan Fisheries Agency and Japan Fisheries Research and Education Agency (2020). Stock assessment and evaluation for Japanese flying squid (fiscal year 2019). 52. Available from: https://abchan.fra.go.jp/wpt/wp-content/uploads/2019/details_2019_19.pdf
- Ji, F., Guo, X., Wang, Y. & Takayama, K. (2020) Response of the Japanese flying squid (*Todarodes pacificus*) in the Japan Sea to future climate warming scenarios. *Climatic Change*, **159**, 601–618.
- Kasahara, S. (1978) Descriptions of offshore squid angling in the sea of Japan, with special reference to the distribution of common squid (*Todarodes pacificus* Steenstrup); and on the techniques for forecasting fishing conditions. *Bulletin of the Japan Sea Regional Fisheries Research Laboratory*, **28**, 179–199.
- Katugin, O.N. (2002) Patterns of genetic variability and population structure in the north pacific squids *Ommastrephes bartramii*, *Todarodes pacificus* and *Berryteuthis magister*. *Bulletin of Marine Science*, **71**, 39.
- Kidokoro, H., Goto, T., Nagasawa, T., Nishida, H., Akamine, T. & Sakurai, Y. (2010) Impact of a climate regime shift on the migration of Japanese common squid (*Todarodes pacificus*) in the sea of Japan. *ICES Journal of Marine Science*, **67**(7), 1314–1322.
- Kidokoro, H., Wada, Y., Shikata, T., Sano, K. & Uji, R. (1999) Growth of the Japanese common squid *Todarodes pacificus* in the sea of Japan in 1996 analyzed from statolith microstructure. *Bulletin of the Japan Sea National Fisheries Research Institute (Japan)*, **49**, 129–135.
- Kim, J.J., Stockhausen, W., Kim, S., Cho, Y.K., Seo, G.H. & Lee, J.S. (2015) Understanding interannual variability in the distribution of, and transport processes affecting, the early life stages of *Todarodes pacificus* using behavioral-hydrodynamic modeling approaches. *Progress in Oceanography*, **138**, 571–583.
- Kim, S.-W., Cho, K.-D., Kim, Y.-S., Choi, Y.-S., Ahn, Y.-H. & Kim, Y. (2005) Distribution of fishing Boats at night in the East Sea derived from DMSP/OLS imagery. *Korean Journal of Fisheries and Aquatic Sciences*, **38**(5), 323–330. Available from: <https://doi.org/10.5657/kfas.2005.38.5.323>
- Kishi, M.J., Nakajima, K., Fujii, M. & Hashioka, T. (2009) Environmental factors which affect growth of Japanese common squid, *Todarodes pacificus*, analyzed by a bioenergetics model coupled with a lower trophic ecosystem model. *Journal of Marine Systems*, **78**(2), 278–287.
- Kiyofuji, H. & Saitoh, S. (2004) Use of nighttime visible images to detect Japanese common squid *Todarodes pacificus* fishing areas and potential migration routes in the sea of Japan. *Marine Ecology Progress Series*, **276**, 173–186.
- Lipiński, M.R., Mwanangombe, C.H., Durholtz, D., Yemane, D., Githaiga-Mwicigi, J. & Sauer, W.H.H. (2020) Age estimates of chokka squid *Loligo reynaudii* off South Africa and their use to test the effectiveness of a closed season for conserving this resource. *African Journal of Marine Science*, **42**(4), 461–471.
- Liu, B.L., Cao, J., Truesdell, S.B., Chen, Y., Chen, X.J. & Tian, S.Q. (2016) Reconstructing cephalopod migration with statolith elemental signatures: a case study using *Dosidicus gigas*. *Fisheries Science*, **82**, 425–433.
- Masuda, D., Kai, S., Yamamoto, N., Matsushita, Y. & Suuronen, P. (2014) The effect of lunar cycle, tidal condition and wind direction on the catches and profitability of Japanese common squid *Todarodes pacificus* jigging and trap-net fishing. *Fisheries Science*, **80**, 1145–1157.
- Miyazawa, Y., Varlamov, S.M., Miyama, T., Guo, X., Hihara, T., Kiyomatsu, K. et al. (2017) Assimilation of high-resolution sea surface temperature data into an operational nowcast/forecast system around Japan using a multi-scale three-dimensional variational scheme. *Ocean Dynamics*, **67** (6), 713–728.
- Mokrin, N.M., Novikov, Y.V. & Zuenko, Y.I. (2002) Seasonal migrations and oceanographic conditions for concentration of the Japanese flying squid (*Todarodes pacificus* Steenstrup, 1880) in the northwestern Japan Sea. *Bulletin of Marine Science*, **71**, 487–499.
- Murata, M. (1990) Oceanic resources of squids. *Marine Behavior and Physiology*, **18**(1), 19–71.
- Nigmatullin, C.M., Nesis, K.N. & Arkhipkin, A.I. (2001) A review of the biology of the jumbo squid *Dosidicus gigas* (Cephalopoda: Ommastrephidae). *Fisheries Research*, **54**(1), 9–19.
- Nishijima, S., Kubota, H., Kaga, T., Okamoto, S., Miyahara, H. & Okamura, H. (2021) State-space modeling clarifies productivity regime shifts of Japanese flying squid. *Population Ecology*, **63**(1), 27–40.

- Oh, Y., Kim, D.-W., Jo, Y.-H., Hwang, J.-D. & Chung, C.-Y. (2020) Spatial variability of fishing grounds in response to oceanic front changes detected by multiple satellite measurements in the East (Japan) sea. *International Journal of Remote Sensing*, **41**, 5884–5904.
- Park, K.-A., Chung, J.Y. & Kim, K. (2004) Sea surface temperature fronts in the East (Japan) sea and temporal variations. *Geophysical Research Letters*, **31**, L07304. Available from: <https://doi.org/10.1029/2004GL019424>
- Piatkowski, U., Pierce, G.J. & Da Cunha, M.M. (2001) Impact of cephalopods in the food chain and their interaction with the environment and fisheries: an overview. *Fisheries Research*, **52**(1–2), 5–10.
- Rigby, P.R. & Sakurai, Y. (2005) Multidimensional tracking of giant Pacific octopuses in northern Japan reveals unexpected foraging behaviour. *Marine Technology Society Journal*, **39**(1), 64–67.
- Rodhouse, P.G., Elvidge, C.D. & Trathan, P.N. (2001) Remote sensing of the global light-fishing fleet: an analysis of interactions with oceanography, other fisheries and predators. *Advances in Marine Biology*, **39**, 261–303.
- Rodhouse, P.G., Pierce, G.J., Nichols, O.C., Sauer, W.H., Arkhipkin, A.I., Laptikhovskiy, V.V. et al. (2014) Environmental effects on cephalopod population dynamics: implications for management of fisheries. *Advances in Marine Biology*, **67**, 99–233.
- Rosa, A.L., Yamamoto, J. & Sakurai, Y. (2011) Effects of environmental variability on the spawning areas, catch, and recruitment of the Japanese common squid, *Todarodes pacificus* (Cephalopoda: Ommastrephidae), from the 1970s to the 2000s. *ICES Journal of Marine Science*, **68**, 1114–1121.
- Sakaguchi, K., Sato, T., Mitsuhashi, M. & Kidokoro, H. (2009) Age and hatching date of Japanese common squid, *Todarodes pacificus*, in waters around Hokkaido. *Nippon Suisan Gakkaishi*, **75**, 204–212 (in Japanese with English abstract).
- Sakurai, Y., Kiyofuji, H., Saitoh, S., Goto, T. & Hiyama, Y. (2000) Changes in inferred spawning areas of *Todarodes pacificus* (Cephalopoda: Ommastrephidae) due to changing environmental conditions. *ICES Journal of Marine Science*, **57**, 24–30.
- Sakurai, Y., Bower, J.R. & Nakamura, Y. (1998) Effect of temperature on development and survival of *Todarodes pacificus* embryos and paralarvae. *Oceanographic Literature Review*, **3**(45), 556.
- Semmens, J.M., Pecl, G.T., Gillanders, B.M., Waluda, C.M., Shea, E.K., Jouffre, D. et al. (2007) Approaches to resolving cephalopod movement and migration patterns. *Reviews in Fish Biology and Fisheries*, **17**, 401–423.
- Sil, S., Miyazawa, Y., Varlamov, S., Waseda, T., & Guo, X. (2012). A high-resolution hindcast of sub-mesoscale Kuroshio-islands-tide interactions in the Izu Islands region, south of Japan. In AGU Fall Meeting Abstracts (Vol. **2012**, pp. OS21A-1667).
- Takayanagi, S. (1993) *Changes in growth and maturity of Japanese common squid (Todarodes pacificus) related to differences in stock size in the Tsugaru Strait, Northern Japan*. Tokyo: Recent Advances in Fisheries Biology, Tokai University Press, pp. 545–553.
- Tian, H., Liu, Y., Tian, Y., Alabia, I.D., Qin, Y., Sun, H. et al. (2022) A comprehensive monitoring and assessment system for multiple fisheries resources in the Northwest Pacific based on satellite remote sensing technology. *Frontiers in Marine Science*, **9**, 808282.
- Waluda, C. & Rodhouse, P. (2006) Remotely sensed mesoscale oceanography of the Central Eastern Pacific and recruitment variability in *Dosidicus gigas*. *Marine Ecology Progress Series*, **310**, 25–32.
- Watanabe, K., Sakurai, Y., Segawa, S. & Okutani, T. (1996) Development of the ommastrephid squid *Todarodes pacificus*, from fertilized egg to the rhynchoteuthion paralarva. *American Malacological Bulletin*, **13**(1/2), 73–88.
- Wei, G., Xinjun, C. & Gang, L. (2018) Interannual variation and forecasting of *Ommastrephes bartramii* migration gravity in the Northwest Pacific Ocean. *Journal of Shanghai Ocean University*, **27**(4), 573–583. Available from: <https://doi.org/10.12024/jsou.20171102171>
- Wijermans, N., Boonstra, W.J., Orach, K., Hentati-Sundberg, J. & Schlüter, M. (2020) Behavioural diversity in fishing—towards a next generation of fishery models. *Fish and Fisheries*, **21**, 872–890.
- Yamaguchi, T., Kawakami, Y. & Matsuyama, M. (2018) Analysis of the hatching site and migratory behaviour of the swordtip squid (*Uroteuthis edulis*) caught in the Japan Sea and Tsushima Strait in autumn estimated by statolith analysis. *Marine Biology Research*, **14**, 105–112.
- Yamamoto, J., Shimura, T., Uji, R., Masuda, S., Watanabe, S. & Sakurai, Y. (2007) Vertical distribution of *Todarodes pacificus* (Cephalopoda: Ommastrephidae) paralarvae near the Oki Islands, southwestern Sea of Japan. *Marine Biology*, **153**, 7–13.
- Yatsu, A., Midorikawa, S., Shimada, T. & Uozumi, Y. (1997) Age and growth of the neon flying squid, *Ommastrephes bartramii*, in the North Pacific Ocean. *Fisheries Research*, **29**, 257–270.
- Yatsu, A., Tafur, R. & Maravi, C. (1999) Embryos and rhynchoteuthion paralarvae of the jumbo flying squid *Dosidicus gigas* (Cephalopoda) obtained through artificial fertilization from Peruvian waters. *Fisheries Science*, **65**, 904–908.
- Zhang, X., Saitoh, S.-I. & Hirawake, T. (2017) Predicting potential fishing zones of Japanese common squid (*Todarodes pacificus*) using remotely sensed images in coastal waters of South-Western Hokkaido, Japan. *International Journal of Remote Sensing*, **38**, 6129–6146.

Supporting Information

Additional supporting information may be found online in the Supporting Information section at the end of the article.

Figure S1. Schematic representation of the migration routes of multiple batches and the fishing grounds.

Figure S2. Schematic representation of the migration routes by (A), Kiyofuji and Saitoh (2004) and (B), Kishi et al. (2009).

Figure S3. Compare between average age of catch (dotted line) and (A) averaged age of harvestable stock estimated by age spectrum (solid line), (B) averaged age of catches estimated by age spectrum (solid line).

Figure S4. Age spectrum of *T. pacificus* in the Japan Sea from 2012 to 2019. Based on model result.

Figure S5. Same of Figure 6 in main text, but for the result of 2012.

Figure S6. Same of Figure 6 in main text, but for the result of 2013.

Figure S7. Same of Figure 6 in main text, but for the result of 2014.

Figure S8. Same of Figure 6 in main text, but for the result of 2015.

Figure S9. Same of Figure 6 in main text, but for the result of 2017.

Figure S10. Same of Figure 6 in main text, but for the result of 2018.

Figure S11. Same of Figure 6 in main text, but for the result of 2019.